Discovery of compounds blocking the proliferation of Toxoplasma gondii and Plasmodium falciparum in a chemical space based on piperidinyl-benzimidazolidinone analogs.

Nadia Saïdani, Cyrille y Botté, Michael Deligny, Anne-Laure Bonneau, Janette Reader, Ronald Lasselin, Goulven Merer, Alisson Niepceron, Fabien Brossier, Jean-Christophe Cintrat, et al.

AAC Journals.ASM.org

Discovery of Compounds Blocking the Proliferation of *Toxoplasma gondii* and *Plasmodium falciparum* in a Chemical Space Based on Piperidinyl-Benzimidazolone Analogs

Nadia Saïdani,[a,b] Cyrille Y. Botté,[a,c] Michael Deligny,[d*] Anne-Laure Bonneau,[d*] Janette Reader,[e] Ronald Lasselin,[e] Goulven Merer,[e] Alisson Niepceron,[f] Fabien Brossier,[f] Jean-Christophe Cintrat,[d] Bernard Rousseau,[d] Lyn-Marie Birkholtz,[e] Marie-France Cesbron-Delauw,[c] Jean-François Dubremetz,[b] Corinne Mercier,[c] Henri Vial,[b] Roman Lopez,[d*] Eric Maréchal[a]

Commissariat à l'Energie Atomique, Centre National de la Recherche Scientifique, Université Grenoble Alpes, Institut National de la Recherche Agronomique, Unité Mixte de Recherche 5168, Institut de Recherches en Technologies et Sciences pour le Vivant, Grenoble, France[a]; Centre National de la Recherche Scientifique, Université Montpellier II, Unité Mixte de Recherche 5235, Montpellier, France[b]; Centre National de la Recherche Scientifique, Université Grenoble Alpes, Unité Mixte de Recherche 5163, Institut Jean Roget, Grenoble, France[c]; Commissariat à l'Energie Atomique, Institut de Biologie et Technologies de Saclay, Laboratoire de Chimie Bioorganique, Gif-sur-Yvette, France[d]; Malaria Research Group, Department of Biochemistry, University of Pretoria, Pretoria, South Africa[e]; Institut National de la Recherche Agronomique, Université de Tours, Unité Mixte de Recherche 1282, Infectiologie Animale et Santé Publique, Centre de Recherche de Tours, Nouzilly, France[f]

A piperidinyl-benzimidazolone scaffold has been found in the structure of different inhibitors of membrane glycerolipid metabolism, acting on enzymes manipulating diacylglycerol and phosphatidic acid. Screening a focus library of piperidinyl-benzimidazolone analogs might therefore identify compounds acting against infectious parasites. We first evaluated the *in vitro* effects of (*S*)-2-(dibenzylamino)-3-phenylpropyl 4-(1,2-dihydro-2-oxobenzo[d]imidazol-3-yl)piperidine-1-carboxylate (compound 1) on *Toxoplasma gondii* and *Plasmodium falciparum*. In *T. gondii*, motility and apical complex integrity appeared to be unaffected, whereas cell division was inhibited at compound 1 concentrations in the micromolar range. In *P. falciparum*, the proliferation of erythrocytic stages was inhibited, without any delayed death phenotype. We then explored a library of 250 analogs in two steps. We selected 114 compounds with a 50% inhibitory concentration (IC_{50}) cutoff of 2 μM for at least one species and determined *in vitro* selectivity indexes (SI) based on toxicity against K-562 human cells. We identified compounds with high gains in the IC_{50} (in the 100 nM range) and SI (up to 1,000 to 2,000) values. Isobole analyses of two of the most active compounds against *P. falciparum* indicated that their interactions with artemisinin were additive. Here, we propose the use of structure-activity relationship (SAR) models, which will be useful for designing probes to identify the target compound(s) and optimizations for monotherapy or combined-therapy strategies.

The phylum *Apicomplexa* comprises a group of unicellular eukaryotes, including obligate intracellular parasites that cause diseases ranging from benign to serious (1). In humans, the most devastating of these infections is malaria, caused by *Plasmodium* parasites, with *Plasmodium falciparum* being the deadliest. Malaria affects about 225 million humans and results in 650,000 deaths every year (2). *Toxoplasma gondii* is another *Apicomplexa* organism that causes toxoplasmosis, affecting one-third of the world population (3). Other parasites, such as *Babesia* spp., *Neospora* spp., and *Eimeria* spp., cause diseases of veterinary importance (4). *Apicomplexa* require large amounts of glycerolipids to build up membrane compartments throughout their life cycle. *Plasmodium* asexual proliferation illustrates this demand. Once invading a hepatocyte, a single sporozoite divides, producing 40,000 merozoites (5). Each merozoite then begins a cycle of schizogonic development inside erythrocytes. As a consequence, a 500 to 700% increase in membrane lipids is observed in infected erythrocytes compared to uninfected ones (6).

The structure of glycerolipids is obtained by the assembly of (i) a 3-carbon glycerol backbone originating from glycerol-3-phosphate (G3P), (ii) fatty acids (FA) esterified at positions *sn* −1 and *sn* −2 in glycerol, and (iii) a polar head at position *sn* −3. It has long been considered that *Apicomplexa* scavenge their fatty acids and glycerolipids from the host (5–8). However, the existence of biosynthetic pathways has been demonstrated, leading to the consensus that *Apicomplexa* meet their actual demand by a combination of scavenging and *de novo* synthesis (9).

The synthesis of glycerolipids is initiated by two acyltransferases generating lysophosphatidic acid (LPA) and phosphatidic acid (PA) (Fig. 1). LPA can be synthesized in the endoplasmic reticulum (ER) by an acyl-CoA:G3P acyltransferase (CoA, coenzyme A) in both *P. falciparum* (10) and *T. gondii*. Genes encoding acyl-CoA:1-acyl-G3P acyltransferases, which catalyze the synthesis of PA in the ER, have been predicted at least in *T. gondii*. Alternatively, PA might be neosynthesized in the apicoplast in both *P. falciparum* and *T. gondii* (11). The second main precursor for glycerolipid synthesis is diacylglycerol (DAG) (Fig. 1), which is

Received 5 July 2013 Returned for modification 15 October 2013
Accepted 8 February 2014
Published ahead of print 18 February 2014
Address correspondence to Eric Maréchal, eric.marechal@cea.fr.
N.S. and C.Y.B. contributed equally to this article.
* Present address: Michael Deligny, UCB Pharma, Brussels, Belgium; Anne-Laure Bonneau, Institut National de la Propriété Industrielle, Courbevoie, France; Roman Lopez, Taj-Deloitte, Paris, France.
This article is dedicated to the memory of our coauthor Fabien Brossier, who sadly passed away in January 2014. We express our deepest condolences to his family, friends, and colleagues at INRA Tours.
Supplemental material for this article may be found at http://dx.doi.org/10.1128/AAC.01445-13.

doi:10.1128/AAC.01445-13

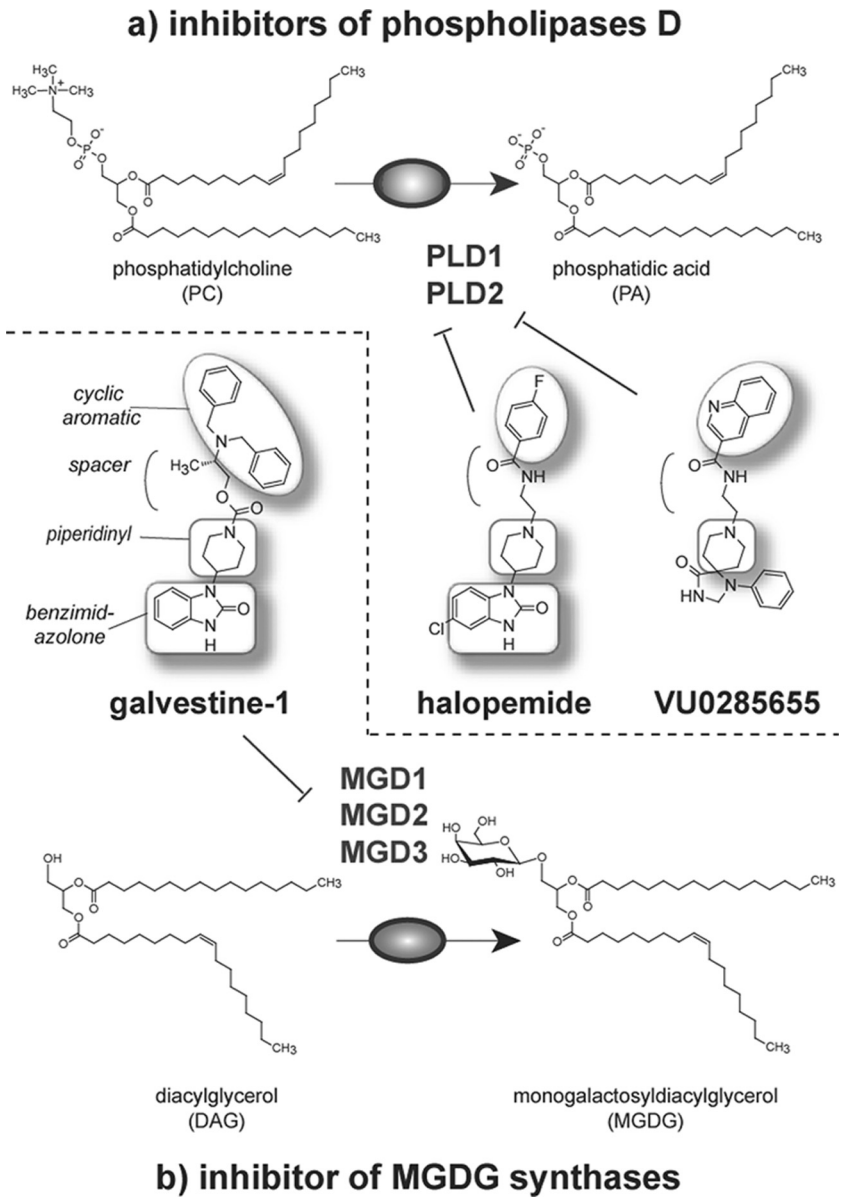

FIG 1 Piperidinyl-benzimidazolones acting on glycerolipid metabolism. Independent reports have shown that 4-(2-oxo-3H-benzimidazol-1-yl)piperidine-1 (or piperidinyl-benzimidazolone) analogs inhibit specifically glycerolipid-manipulating enzymes. (a) Chemical structures of halopemide (PubChem ID CID 65490) and VU0285655. *N*-[2-[4-(5-chloro-2-oxo-3H-benzimidazol-1-yl)piperidine-1-yl]ethyl]-4-fluorobenzamide was shown to selectively inhibit mammal phospholipases D (in humans, PLD1 and PLD2) (41, 42). An exploration of the chemical space of halopemide analogs has shown that compounds can be equally efficient on PLD1 and PLD2 or more specific to one or the other. Halopemide and halopemide analogs therefore inhibit the conversion of PC into PA. Compounds with a 1-phenyl-1,3,8-triazaspiro[4,5]decan-4-one scaffold, such as VU0285655 (PubChem ID CID 44138050), exhibit a higher selectivity for PLD2 (42, 43). (b) Chemical structure of galvestine-1. [(2S)-2-(dibenzylamino)propyl] 4-(2-oxo-3H-benzimidazol-1-yl)piperidine-1-carboxylate (PubChem ID CID 25192811) was shown to selectively inhibit plant MGDG synthases (three isoforms in *A. thaliana*, MGD1, MGD2, and MGD3) by competition with DAG (23, 40).

neosynthesized by the hydrolysis of PA by a phosphatidate phosphatase (PAP). At least two genes are predicted to encode PAPs in *P. falciparum* and *T. gondii*. Conversely, DAG can be phosphorylated into PA by diacylglycerol kinases (DGK) in both *P. falciparum* and *T. gondii*. PA and DAG can also be generated from existing phospholipids via the action of phospholipase D (PLD) and phospholipase C (PLC), respectively. Although PLDs and PLCs are widely represented in eukaryotes, only one gene has been demonstrated to encode a PLC in *P. falciparum* (12) and *T. gondii* (13). To our knowledge, no PLD has been characterized in any *Apicomplexa* parasite.

DAG and PA serve as precursors for all membrane glycerolipids. In eukaryotes, two main subcellular compartments are responsible for the synthesis of complex glycerolipids: one is the ER, synthesizing phospholipids, and the other one is the plastid of photosynthetic organisms, synthesizing nonphosphated glycoglycerolipids, including monogalactosyldiacylglycerol (MGDG). Although the apicoplast derives from a photosynthetic plastid (14), no enzyme synthesizing glycoglycerolipids was identified in this organelle (15, 16).

Given the importance of glycerolipids for membrane biogenesis, their metabolism appears to be a potential target for novel treatments. Taking the available data summarized above, the bio-

synthesis of glycerolipids is therefore constituted of 3 metabolic segments: (i) the neosynthesis/scavenging of FAs, (ii) the PA↔DAG hub, and (iii) the synthesis of phospholipids from PA and DAG. In the first metabolic segment, the synthesis of FAs in the apicoplast by FA synthase (FAS) II has inspired numerous attempts to develop novel drugs (for a review, see 9 and 17), but erythrocytic stages of *P. falciparum* were shown to survive without a functional *de novo* synthesis (5, 18, 19), and the efficacy of anti-FAS II drugs against the blood stages is likely due to off-target effects (9). In the third metabolic segment, the synthesis of glycerophospholipids, and particularly phosphatidylcholine, was shown to be a valid target: chemical scaffolds like thiazolium analogs of choline (20, 21) or phospholipid structural analogs, like PG12 (22), have been proposed to be novel classes of efficient antiparasitic drugs. No drug has been developed to target the second metabolic segment, i.e., at the level of the PA↔DAG hub. In this article, we explore the chemical space of piperidinyl-benzimidazolone analogs of galvestine-1 (a competitor of DAG binding on MGDG synthases) and halopemide (an inhibitor of PLDs producing PA) (Fig. 1) to search for novel classes of compounds acting on the proliferation of *T. gondii* and *P. falciparum*.

MATERIALS AND METHODS

Library of piperidinyl-benzimidazolone analogs. The library used in this work was described previously (23). The structures are given in Table S1 in the supplemental material. The compounds were synthesized and analyzed by liquid chromatography and nuclear magnetic resonance (NMR). High-pressure liquid chromatography was performed using a Waters system (2525 binary gradient module, in-line degasser, 2767 sample manager, and 2996 photodiode array detector). Analytical reverse-phase (RP) high-pressure liquid chromatography (HPLC) was achieved with an X-bridge C_{18} column (100 by 4.6 mm, 3.5-μm particle size, and 135-Å pore size) at a 1-ml/min flow rate. Preparative RP-HPLC was achieved with an X-bridge C_{18} column (150 by 19 mm, 5-μm particle size, and 135-Å pore size) at a 17-ml/min flow rate. Elution was carried out with a gradient of A (99.9% water/0.1% HCOOH) and B (99.9% acetonitrile [ACN]/0.1% HCOOH). Mass spectra were obtained on a Waters Micromass ZQ system with a ZQ2000 quadrupole analyzer. The ionization was performed by electrospray with a source temperature of 120°C, a cone voltage of 20 V, and continuous sample injection at a 0.3-ml/min flow rate. Mass spectra were recorded in positive ion mode in the *m/z* 100 to 2,000 range and treated with the MassLynx 4.0 software. NMR experiments were performed on a Bruker Avance 400 Ultrashield (Karlsruhe, Germany). The spectra were recorded at room temperature at 400 MHz for ^{1}H NMR and 100 MHz for ^{13}C. The samples were dissolved in cyclohexane-ethyl acetate (7:3 [vol/vol]) at a concentration of 5 mM. The chemical shifts are given in ppm and the coupling constants in Hz. (Chemical characterizations and commercial sources are given in the supplemental material for a subset of compounds analyzed more carefully than described here.) The average purity is 93.34% (minimum to maximum, 90 to 99). In accordance with the Lipinski rules, the compounds had, on average, 0.86 H-bond donors (minimum to maximum, 0 to 4), 4.47 H-bond acceptors (minimum to maximum, 2 to 9), an average molecular weight of 537 (minimum to maximum, 217 to 844), and an average logP of 5.18 (minimum to maximum, 0.47 to 9.71). All compounds were solubilized in dimethyl sulfoxide (DMSO) and stored at −20°C until use.

***T. gondii* culture in human foreskin fibroblasts.** *T. gondii* RH and RH-β1 strains were maintained by serial passages in a confluent human foreskin fibroblast (HFF) monolayer, as described previously (24, 25). The RH-β1 strain carries the *Escherichia coli lacZ* (β-galactosidase) gene under the control of the SAG1 promoter (26). The cultures were maintained in Dulbecco's modified Eagle medium (DMEM) containing L-glutamine supplemented with 10% fetal bovine serum (FBS) and antibiotics (10,000 U · ml^{-1} penicillin and 10 mg · ml^{-1} streptomycin) (Gibco, Invitrogen Corporation, United Kingdom) at 37°C with 5% CO_2. Imaging was performed using an Axioplan 2 microscope and an AxioCam MRn camera (Zeiss).

***In vitro* assay of *Toxoplasma* proliferation by colorimetric titration.** Microtiter plates (96 wells) were seeded with HFF cells and allowed to grow to confluence in DMEM containing L-glutamine, 10% FBS, and antibiotics (10,000 U · ml^{-1} penicillin, 10 mg · ml^{-1} streptomycin) at 37°C with 5% CO_2. *T. gondii* cells used in the 50% inhibitory concentration (IC_{50}) assay were prepared as follows: a culture of RH-β1 that had completely lysed HFF monolayers was forced through a 27-gauge needle twice and then filtered through a 3-μm-pore-size filter. The flowthrough was centrifuged at 250 × *g* for 10 min to collect the parasites, which were washed once in 5 ml phosphate-buffered saline (PBS). The parasites were resuspended in PBS and counted (25). HFF cell monolayers grown in 96-well microtiter plates were infected with 10^4 parasites per well (200 μl) and incubated on ice for 15 min to allow parasite sedimentation and promote synchronization for invasion. The parasites were allowed to invade for 15 min at 37°C with 5% CO_2. The wells were rinsed three times with PBS. Intracellular parasites were allowed to grow in the absence (controls) or presence of a range of compound concentrations (1 nM to 500 μM). The controls were grown in DMEM with or without DMSO. Each assay was carried out in triplicate. The plates were incubated at 37°C with 5% CO_2 for 48 to 72 h to allow parasite development until the control wells were fully lysed (27). The β-galactosidase activity was measured as described earlier (26). The plates were read at 570 and 630 nm on a Bio-Tek microtiter plate reader. The results are presented as the mean ± 2 standard errors of the mean. Triplicates of the standard curve experiments were carried out in parallel by infecting another 96-well plate with serial dilutions of the corresponding parasite strain (0 to 10^7 parasites/well).

***Toxoplasma* motility assay.** The assay is based on the deposition of surface proteins (SAG1) after the gliding of *T. gondii* on a glass slide (28). Glass slides were coated with poly-D-lysine (10 μg · ml^{-1} in PBS) for 1 h at 37°C and washed with PBS. Freshly purified tachyzoites (10^7) were preincubated with or without the tested compound and deposited onto the surface of a coated slide. After 10 min at room temperature, the excess liquid was removed, 500 μl of poly-D-lysine (10 μg · ml^{-1} in D10 medium) was added, and the slide was incubated for 25 min at 37°C. The gliding trails were visualized by immunofluorescence using an anti-SAG1 antibody (29, 30) at 1:500, followed by a 45-min incubation with a Texas Red coupled goat anti-mouse IgG (H+L) (1:1,000; Molecular Probes; Invitrogen). The labeled gliding trails were visualized using an epifluorescence Axioplan 2 microscope (Zeiss) after excitation at 596 nm and capture of emission at 620 nm, using an AxioCam MRn camera (Zeiss).

***Toxoplasma* apical complex integrity.** The apical complex integrity was concisely assayed by analyzing the *in vitro* induction of the extrusion of the conoid by Ca^{2+} ionophores and the secretion of MIC2 by micronemes induced by ethanol. For the conoid extrusion assay, 10^5 freshly purified tachyzoites were preincubated with or without the tested compound and incubated with 1 μM ionomycin, as described earlier (31). To test the ethanol-induced secretion of MIC2, 10^9 freshly purified tachyzoites were preincubated with or without tested compound, washed three times with PBS, and suspended in FBS 0.1% in PBS (pH 7.4). Ethanol was added at a 1% final concentration, and the parasites were incubated for 1 h at 37°C (32). The parasites were then separated from the microneme content by centrifugation at 2,000 × *g*. The supernatant was collected and analyzed by SDS-PAGE, electrotransfer, and Western blotting using anti-MIC2 antibodies (monoclonal antibody [MAb] T3.4A11.2b4; 1:5,000 dilution) and a secondary mouse antibody coupled with peroxidase and revealed by chemiluminescence (ECL kit; Millipore). The anti-GRA1 antibody (MAb Tg17.43.1; 1:5,000 dilution) (33) was used as a control.

***P. falciparum* culture.** Experiments were performed using chloroquine-sensitive (3D7 and Nigerian) or chloroquine-resistant (W2, FCM29, and Dd2) *P. falciparum* strains, as indicated in Results. For sys-

tematic screening, we used the 3D7 strain. The strains were maintained in continuous culture in human erythrocytes, according to the method of Trager and Jensen (34).

Standard evaluation of *in vitro* antimalarial activity. *In vitro* antimalarial activity was measured using asynchronous 3D7 chloroquine-sensitive *P. falciparum*-infected red blood cells (RBC). Suspensions of infected RBC at 1.5% final hematocrit and 0.6% parasitemia were cultured in complete medium (RPMI 1640 complemented with 25 mM HEPES [pH 7.4] and 0.5% AlbuMAX I) in the absence (controls) or presence of compounds, according to the procedure outlined by Desjardins et al. (35). The compounds were dissolved in DMSO at 10 mM and then diluted in culture medium so that the final DMSO concentration was never >0.5%. After a 48-h (length of the parasite's cycle) or 96-h incubation (as indicated in Results), 0.5 μCi [^{3}H]hypoxanthine was added to each well. After 18 h of incubation at 37°C, the cells were lysed, and the parasite macromolecules, including radioactive nucleic acids, were retained on glass fiber filters. Emissions from the radiolabeled material were counted (Tri-Carb 2900TR scintillation counter). The radioactive background was obtained after incubation of noninfected red blood cells under the same conditions. Analyses of dose-effect curves were performed with the GraphPad Prism analytical software. The drug effects were expressed as the IC_{50} values. The results are the means of at least two independent experiments (different cell cultures and different compound dilution stocks), each performed in duplicate.

Drug effects during the *P. falciparum* erythrocyte cycle. The parasites were synchronized twice by 5-min treatments with sorbitol 5% and washing with RPMI, a process allowing for the selection of ring stages. Infected RBC (1% final hematocrit, 0.6% parasitemia, 1.5 ml) were then grown in presence or absence of compounds. To evaluate the effects at different stages of the parasitic cycle, the compounds were added at 4 h for the ring stage, 20 h for the trophozoite stage, or 32 h for the schizont stage (following the second sorbitol treatment). After 4 h of incubation with the compounds, the parasites were washed and resuspended in fresh medium without drugs. At 52 h, 0.5 μCi [^{3}H]hypoxanthine was added. The reactions were stopped at 75 h by freezing the plate at −80°C, and the cells were lysed and filtered as described above to determine the IC_{50}s of the compounds.

Isobolograms for the evaluation of interactions between selected compounds and artemisinin against *P. falciparum*. To examine the *in vitro* interaction of compounds 8 and 12 with artemisinin, isobolograms were constructed as described earlier (36). Concentrations of each compound were expressed as fractional inhibitory concentrations (FIC), which is the fraction of IC_{50} of a compound when tested alone. The isobolograms were constructed by plotting the FIC for the tested compounds versus the FIC for artemisinin. A drug combination is considered synergistic if the sum of the two FIC values for a given combination (ΣFIC) is <0.5 or antagonistic when the ΣFIC is >2 (37) or 4 (38, 39). The nature of the interaction between drugs with ΣFIC values between 0.5 and 2 (or 4) should be considered indifferent (38), i.e., simply additive.

***In vitro* effects of compounds on human cells.** Human lymphoblasts (Jurkat), erythroblasts (K-562), monocytes (THP-1), and macrophages (U-937) were seeded in 200 μl in complete medium (RPMI 1640 complemented with 10% fetal calf serum [FCS], 1% glutamine, 1% penicillin-streptomycin) in 96-well microplates (8,000 cells per well) and incubated 24 h at 37°C and 5% CO_2 in the presence of various concentrations of the tested molecules. [^{3}H]Thymidine (0.5 μCi) was then added, followed by a supplementary incubation of 6 h. The reaction was stopped by congelation at −80°C. Radioactive incorporations into nucleic acids were measured by scintillation counting after collection on glass fiber filters. Radioactive background was measured from complete medium and subtracted from each corresponding well. The IC_{50} is the drug concentration that led to 50% cell growth inhibition. In the case of human hepatocellular liver carcinoma cells (HepG2), the cells were seeded in DMEM (supplemented with 10% [vol/vol] heat-inactivated FBS and 1% penicillin-streptomycin at 37°C, 5% CO_2, 90% humidity, and 10^5 cells per well) and grown for 24 h at 37°C in the presence of various concentrations of tested molecules. Cell viability was measured using the lactate dehydrogenase (LDH) assay (BioVision) by transferring 10 μl of the supernatant to a new 96-well plate and adding 100 μl LDH reaction mix (BioVision), incubation for 30 min at room temperature, and measuring the LDH activity through absorbance at 450 nm. Cell viability was expressed as a percentage of the control. Analyses of dose-effect curves were performed with the GraphPad Prism analytical software. The IC_{50} values were graphically determined from at least two independent experiments (different cell cultures and different compound dilution stocks) performed in duplicate.

RESULTS

Selection of the library of piperidinyl-benzimidazolone analogs. Independent studies have shown that analogs of 4-(2-oxo-3H-benzimidazol-1-yl)piperidine-1 (or piperidinyl-benzimidazolone) might specifically inhibit DAG- or PA-manipulating enzymes. On one hand, [(2S)-2-(dibenzylamino)propyl] 4-(2-oxo-3H-benzimidazol-1-yl)piperidine-1-carboxylate (or galvestine-1; PubChem ID CID 25192811) was shown to selectively inhibit plant MGDG synthases (3 isoforms in *Arabidopsis thaliana*, MGD1, MGD2, and MGD3) by competition with DAG (23, 40) (Fig. 1). On the other hand, *N*-(2-(4-(5-chloro-2-oxo-1-benzimidazolinyl)piperidino)ethyl)-p-fluorobenzamide (or halopemide; PubChem ID CID 65490) was shown to selectively inhibit mammalian phospholipase D enzymes (in humans, PLD1 and PLD2) (41, 42) (Fig. 1). Inhibition studies of truncated PLD1 support that halopemide analogs act by direct binding to the catalytic site, in which phosphatidylcholine (PC) is hydrolyzed into PA. An exploration of the chemical space of halopemide analogs further showed that compounds were equally efficient on PLD1 and PLD2 or more specific to one or the other. Thus, compounds with a 1-phenyl-1,3,8-triazaspiro[4,5]decan-4-one scaffold, like VU0285655 (PubChem ID CID 44138050), exhibit a higher selectivity for PLD2 (42, 43). Chemical tuning of the piperidinyl-benzimidazolone scaffold can therefore determine the target specificities of the obtained small molecules.

Based on (i) the central roles of DAG and PA in membrane glycerolipid metabolism and function, (ii) the evidence that piperidinyl-benzimidazolone analogs might compete with DAG or bind to the catalytic site of PLD for PC hydrolysis into PA, and (iii) the idea to use halopemide analogs for therapeutic purposes, we designed a library of 250 compounds to explore analogs of piperidinyl-benzimidazolone (structures are shown in Table S1 in the supplemental material). We searched for compounds that might interfere with the enzymes of glycerolipid metabolism, which manipulate the DAG-PA structure. The design of the library is based on chemical substitutions at the level of four diversification points in the structure of the molecules. These diversification points were termed "A" for the benzimidazolone end, "B" for the piperidinyl part, "C" for the substituted di-/tribezylamino ethoxy end, and "spacer" for the initial carboxylate segment between B and C (Fig. 2a). Figure 2 illustrates some families of compounds from this library, allowing testing features responsible for selectivity in galvestine-1, halopemide, and VU0285655. One family was designed to contain only the A1B1 scaffold shared by galvestine-1 and halopemide, including some compounds, like 5 and 6, with part C designed after that of VU285655 (Fig. 2b). Another family contains analogs whose structure contains a B1C1 structure, as found in galvestine-1, with substitutions at the C domain, i.e., the 4-(2-oxo-3H-benzimidazol-1-yl)piperidine-1 part (Fig. 2c). Other families of compounds are characterized by parts A and B

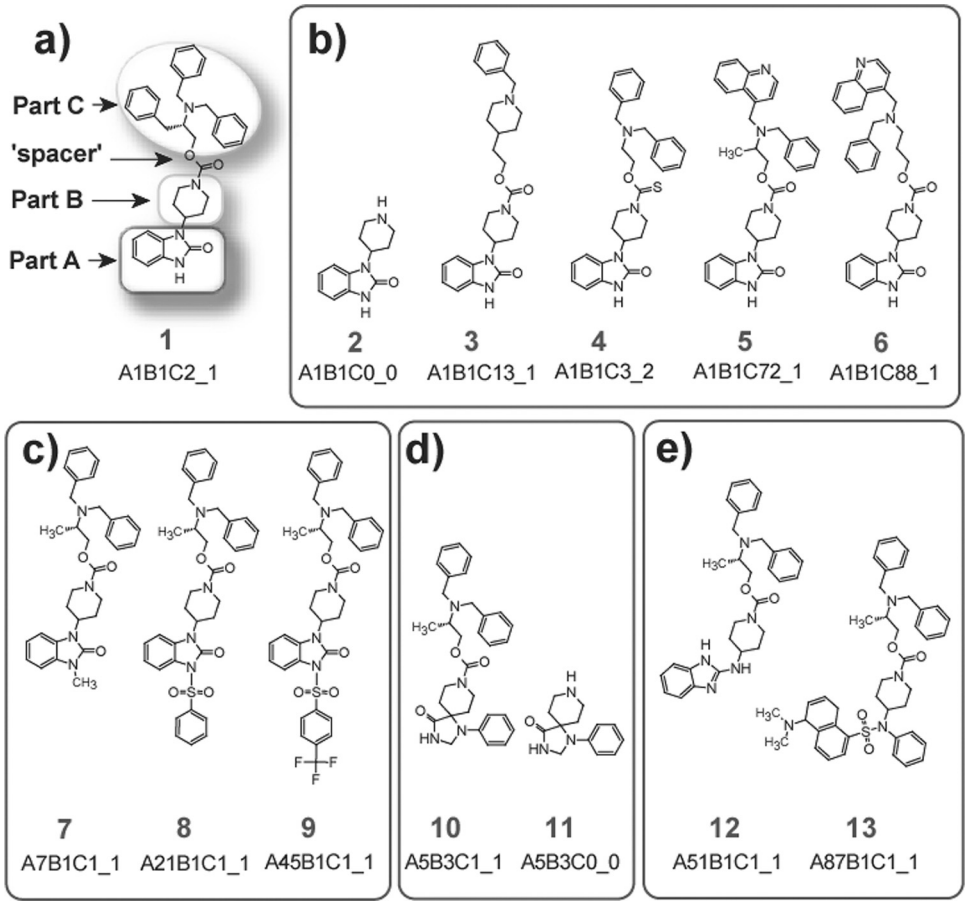

FIG 2 Illustration of compounds in the selected library of piperidinyl-benzimidazolone analogs. (a) Regions of the chemical structure subjected to variations. The chemical structures in the library have been dissected in four parts, illustrated on compound 1: "A" for the benzimidazolone end, "B" for the piperidinyl part, "C" for the substituted di/tribenzylamino ethoxy end, and "spacer" for the initial carboxylate segment between B and C. (b) Examples of compounds with a nonsubstituted 4-(2-oxo-3H-benzimidazol-1-yl)piperidine-1. Compound 2 represents the minimal structure. Compound 3 contains a part C shared with halopemide. Compounds 5 and 6 contain a part C designed after that of VU285655. (c) Examples of compounds (7 to 9) with substitution at the level of 4-(2-oxo-3H-benzimidazol-1-yl)piperidine-1. (d) Examples of compounds (10 and 11) with parts A and B containing 1-phenyl-1,3,8-triazaspiro[4,5]decan-4-one scaffold also found in the structure of VU0285655. (e) Examples of compounds (12 and 13) with strong changes in parts A and B. All compounds are identified by an A#B#C#_# nomenclature following initial syntheses of compounds in the library. All structures of the library are shown in Table S1 in the supplemental material.

containing 1-phenyl-1,3,8-triazaspiro[4,5]decan-4-one scaffold, like VU0285655 (Fig. 2d), and compounds with significant changes in parts A and B (Fig. 2e).

***In vitro* analysis of (*S*)-2-(dibenzylamino)-3-phenylpropyl 4-(1,2-dihydro-2-oxobenzo[d]imidazol-3-yl)piperidine-1-carboxylate (compound 1) on *T. gondii*, *P. falciparum*, and human cells. (i) *In vitro* effects of compound 1 on *T. gondii* tachyzoites.** To investigate whether piperidinyl-benzimidazolones might possess pharmacological potential against *Apicomplexa*, we initially tested galvestine-1 and an analog, (*S*)-2-(dibenzylamino)-3-phenylpropyl 4-(1,2-dihydro-2-oxobenzo[d]imidazol-3-yl)piperidine-1-carboxylate (compound 1) before exploring a more complete library. The compounds were assessed against *T. gondii* and *P. falciparum*. Both compounds inhibited the *in vitro* proliferation of *T. gondii* and *P. falciparum* with IC_{50}s of <15 μM. The most potent inhibitor was compound 1, inhibiting *T. gondii* proliferation with an $IC_{50Toxoplasma}$ of 4.8 μM (Fig. 3a) and *P. falciparum* with an $IC_{50Plasmodium}$ of 1.45 μM (Fig. 3c). We then decided to perform a preliminary investigation of the mechanism of action of compound 1 on parasites and the potential cytotoxicity to human cells *in vitro*.

Figure 3 illustrates the results of our preliminary study on the effects on the development of *T. gondii* and *P. falciparum*. In the experiment, which was designed to determine the IC_{50} of compound 1 against *T. gondii* (Fig. 3a), we noticed that the treatment of intracellular tachyzoites led to an overall reduction of parasitophorous vacuoles and a decrease in the number of parasites per vacuole (see also Fig. 3b). The successful development of tachyzoites can be summarized as a series of obligatory steps, i.e., gliding of the parasites, attachment to the host cell, conoid extrusion, active invasion with formation of a tight junction, sequential secretion of proteins from micronemes and rhoptry neck, formation of a parasitophorous vacuole, and reprogramming of the host cell and intravacuolar division by endodyogeny. Compound 1 had no visible effect on gliding capacities based on an *in vitro* motility assay (see Fig. S1 in the supplemental material). Compound 1 did not inhibit the *in vitro* extrusion of the conoid induced by ionomycin (31), and we did not observe any effect on the microneme secretion-induced ethanol (32) (data not shown).

We sought to determine whether the treatment with compound 1 affects the intracellular proliferation of *T. gondii* tachyzoites using direct observation by phase-contrast micros-

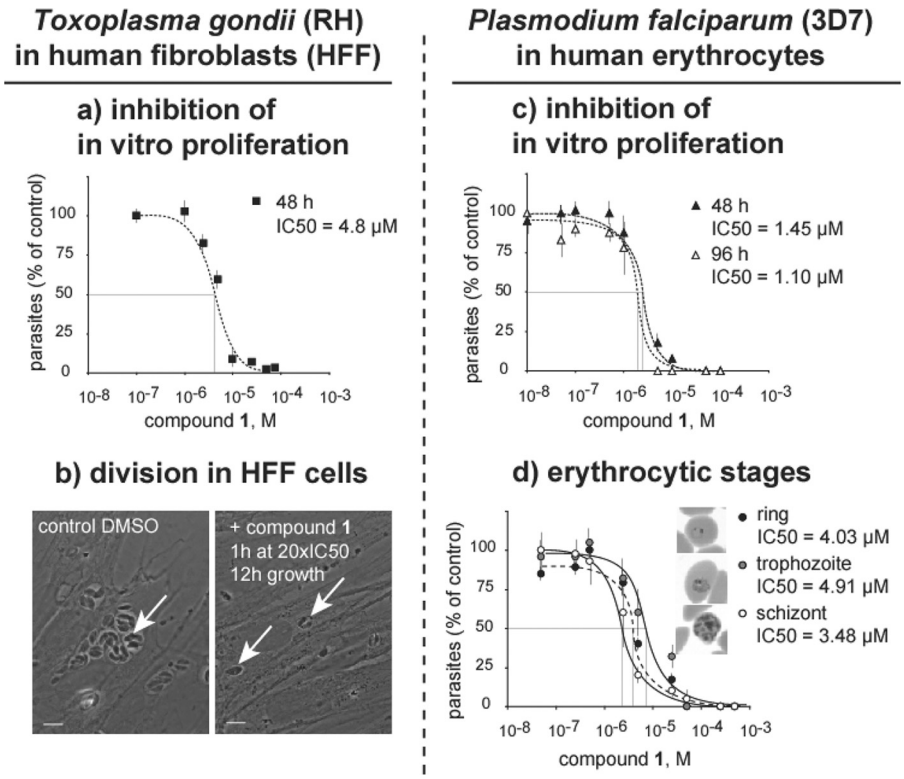

FIG 3 Preliminary analysis of the *in vitro* antiparasitic properties of compound 1, harboring the benzimidazolone-piperidinyl chemotype, on *T. gondii* and *P. falciparum*. Compound 1 was selected for a concise and preliminary analysis of the potential effects of the benzimidazolone-piperidinyl chemotype on *T. gondii* (RH strain) and *P. falciparum* (3D7 strain) at its blood stages, based on an IC_{50} of <5 μM in both models. *T. gondii* was grown in human fibroblasts (HFF cells) and *P. falciparum* in human erythrocytes. (a and b) Effects of compound 1 on *T. gondii*. (a) Effect of compound 1 on proliferation of parasites. IC_{50}s were determined on RH strain grown in HFF cells. (b) Effect on intracellular division of tachyzoites. The parasites were grown in HFF cells. Parasitophorous vacuoles containing 8 to 32 parasites under control conditions or 1 to 2 parasites after treatment are indicated by white arrows. Scale bar, 1 μm. (c and d) Effect of compound 1 on *P. falciparum*. (c) Effect of compound 1 on proliferation of parasites. IC_{50}s were determined on 3D7 strain grown in red blood cells. IC_{50}s were determined after one (at 48 h [▲]) or two (at 96 h [△]) cell divisions so as to detect any delayed cell death phenotype due to an impairment of the apicoplast. (d) Effect of compound 1 on erythrocytic stages. IC_{50}s were determined in synchronized parasites' culture. Captions illustrate ring, trophozoite, and schizont stages. Scale is given by red blood cell radius, i.e., 7 μm. IC_{50}s are indicated with dotted lines in the graphs.

copy and parasite numeration. Tachyzoites were treated for 1 h with compound 1 at concentrations ranging from IC_{50} to 20× IC_{50}. The parasites were then allowed to invade HFF host cells and were grown for 12 h before observation and cell counting. Figure 3b shows that the number of parasites strongly decreased after treatment with compound 1. After 12 h under control conditions, *Toxoplasma* cells reached a number of 8 to 32 parasites per parasitophorous vacuole. In contrast, when parasites were treated for 1 h in the presence of compound 1 prior to HFF infection, the numbers of parasitophorous vacuoles per field and of parasites per vacuole decreased with increasing concentrations of the compound. At 20× IC_{50}, corresponding to an absence of proliferation following the colorimetric titration assay, the number of vacuoles was nevertheless 35% of the control, with parasitophorous vacuoles containing only 1 to 2 parasites each (Fig. 3b). When compound 1 was supplied after the invasion of HFF cells, similar results were obtained. Based on this initial study, we concluded that the effect of compound 1 was likely attributable to a deleterious effect during the cellular division of *Toxoplasma*.

(ii) *In vitro* effects of compound 1 on *P. falciparum* blood stages. We briefly investigated the effect of compound 1 on two features of the erythrocytic life stage of *P. falciparum*. First, we considered that important processes of glycerolipid metabolism occur in two compartments of the cell, i.e., the ER and the apicoplast (see the introduction). It has been shown that most drugs affecting apicoplast maintenance induced a delayed death phenotype, i.e., one that occurred after two full division cycles (9, 44, 45). In *P. falciparum* blood stages, a delayed death effect can only be observed after two full intraerythrocytic cycles, around 96 h postinfection (46, 47). We analyzed the effect of treatment with increasing doses of compound 1 after 48 h and 96 h of *P. falciparum* 3D7 development and did not detect any significant change (Fig. 3c). This result suggests that apicoplast maintenance is not impaired by compound 1.

During the *P. falciparum* blood stage, glycerolipid synthesis is highest during the late stages of development, i.e., the mid-trophozoite and schizont stages, when the biogenesis of daughter cell compartments occurs (48). Since the IC_{50} of the tested piperidinyl-benzimidazolone analog was determined on asynchronous cultures, it was not possible to evaluate the activities on the different intraerythrocytic stages. Thus, we measured the IC_{50} of compound 1 on synchronized ring, trophozoite, and schizont cultures. Compound 1 was similarly active against early stage (ring) and mature stages (trophozoite and schizont) (Fig. 3d).

We investigated the effect of compound 1 on various strains of *P. falciparum* that are sensitive (Nigerian and 3D7) or resistant

TABLE 1 Inhibitory properties of compound 1 on various strains of *Plasmodium falciparum*[a]

	Average IC_{50} (M) of:			
	Chloroquine-sensitive strain:		Chloroquine-resistant strain:	
Antimalarial	Nigerian	3D7	W2	Dd2
Compound 1	1.20×10^{-5}	1.45×10^{-6}	1.05×10^{-6}	1.35×10^{-6}
Chloroquine	3.20×10^{-8}	1.03×10^{-8}	9.90×10^{-8}	1.72×10^{-7}
Artemisinin	ND[b]	2.87×10^{-8}	ND	6.30×10^{-8}
Artesunate	ND	9.70×10^{-9}	ND	1.16×10^{-8}
Triclosan	ND	1.55×10^{-6}	ND	2.10×10^{-6}

[a] Assays were performed using chloroquine-sensitive (Nigerian, 3D7) or resistant (W2, Dd2) strains. The IC_{50}s of other antimalarials (chloroquine, artemisinin, artesunate, and triclosan) were determined in parallel experiments. Each value is the average from two independent experiments.
[b] ND, not determined.

TABLE 2 Inhibitory properties of compound 1 on the *in vitro* proliferation of various human cell models[a]

	Average IC_{50} (M) for:			
Antimalarial	Jurkat	K-562	THP-1	U-937
Compound 1	1.74×10^{-4}	1.99×10^{-5}	1.48×10^{-5}	2.62×10^{-4}
Chloroquine	ND[b]	1.10×10^{-5}	ND	ND
Artemisinin	ND	1.00×10^{-4}	ND	ND
Artesunate	ND	1.06×10^{-6}	ND	ND
Triclosan	ND	1.34×10^{-5}	ND	ND

[a] Lymphoblasts (Jurkat), erythroblasts (K-562), monocytes (THP-1), and macrophages (U-937) were subjected to various concentrations of compound 1 in order to determine the IC_{50} of toxicity based on cell proliferation. The IC_{50}s of other antimalarials (chloroquine, artemisinin, artesunate, and triclosan) were determined in parallel experiments. Each value is the average from two independent experiments.
[b] ND, not determined.

(W2 and Dd2) to chloroquine. Table 1 shows that the IC_{50} of compound 1 was in the 1 to 10 μM range. In the 3D7 strain, we compared the IC_{50} of compound 1 with that of antimalarials known to be active *in vitro* and *in vivo*, i.e., chloroquine, artemisinin, and artesunate (all with IC_{50}s in the 10 nM range in our *in vitro* system) (Table 1) and triclosan, which is known to be efficient only *in vitro* (in the micromolar range) (Table 1).

(iii) *In vitro* cytotoxicity of compound 1 on human cell models and determination of an *in vitro* selectivity index. Since targets of piperidinyl-benzimidazolones may be shared between the parasites and their human host cells, pharmacological activity might be totally or partly due to a nonspecific cytotoxic effect. Before exploring a library of piperidinyl-benzimidazolone analogs, we analyzed the inhibitory properties of compound 1 on various proliferating human cell models. As an initial investigation, we assessed the effect of piperidinyl-benzimidazolones on the morphology and the proliferation of *T. gondii* host cells, i.e., confluent or proliferative HFF cells (not shown). A 12-h treatment with high concentration of compound 1 (100 μM) had no effect on the cytoskeleton integrity of HFF, as observed by light microscopy and immunofluorescence assays (using microtubule, actin, and focal adhesion point probes, i.e., anti-tubulin antibodies, phalloidin, and anti-vinculin antibodies, respectively; not shown). Similarly, compound 1 did not have any effect on the division of growing HFF cells when treated at 50 or 100 μM for 24 h. We then set up a protocol to address the cytotoxicity of compound 1 on more versatile/sensitive human cells. Table 2 shows that compound 1 inhibited the growth of erythroblast (K-562) and monocyte (THP-1) cell lines with IC_{50}s ranging from 15 to 20 μM and the growth of both lymphoblast (Jurkat) and macrophage (U-937) cell lines with IC_{50}s of >170 μM. There is therefore >1 log between the effect on parasites and that on human cells, indicating a relative selectivity of compound 1.

Taking K-562 cells as a standard model for comparison, we calculated a selectivity index (SI), defined as the IC_{50} value determined on a human cell model (cytotoxicity) divided by the IC_{50} value determined on parasites. Table 3 shows that using this standard cell model, we determined an SI for compound 1 of 13.72 on *P. falciparum* and 3.43 on *T. gondii*.

Two-step exploration of the library of piperidinyl-benzimidazolone analogs. The exploration of the library was performed in two steps, so as to select compounds with lower IC_{50}s against *T. gondii* or *P. falciparum* and improved SIs. In the first step, we analyzed the effects of the 250 compounds on the *in vitro* proliferation of both parasites and determined the corresponding IC_{50}s (see Table S1 in the supplemental material). We selected the 114 compounds having an *in vitro* antiparasitic effect with an IC_{50} of ≤2 μM for at least one parasitic model. Figure 4a shows that some compounds (i) had more powerful effects against *T. gondii*, with IC_{50}s in the 100 to 200 nM range (e.g., compounds 4 and 7), (ii) had more potent effects against *P. falciparum*, also in the 100 to 200 nM range (e.g., compounds 8 and 12), and (iii) eventually were equally efficient against both parasites (e.g., compound 13). We did not detect any strong correlation between the IC_{50} values measured on *T. gondii* and *P. falciparum*.

In the second step, we determined the *in vitro* toxicities of the 114 selected compounds on human K-562 erythroblasts (see Table S2 in the supplemental material). The $IC_{50K\text{-}562}$ values allowed us to calculate SIs. Figure 4b shows a plot of the SIs determined for each compound on *Toxoplasma* and *Plasmodium*. The compounds with the lowest values have higher adverse effects in this standard assay, and the compounds with the highest values are likely to be selective to the parasites. The chemical library we explored allowed for the identification of compounds with better properties than the initial compound 1. Compounds 4 and 7 acted more specifically against *T. gondii*, compounds 8 and 12 acted more specifically against *P. falciparum*, and compound 13 acted on both parasites; these also displayed improved SIs (Fig. 4b).

Remarkably, the SIs of compounds 4 and 7 for *T. gondii* (versus mammalian cells) were 488 and 275, respectively (Table 3). These values are promising for the development of antitoxoplasmic drug candidates. The SI values of compounds 8 and 12 relative to *P. falciparum* were 1,078 and 74, close to the SI values obtained with chloroquine or artesunate (1,068 and 109, respectively), which were measured in parallel using our assay, and were lower than that of artemisinin, i.e., 3,484 (Table 3). Additionally, the SIs of these compounds were determined against human hepatocellular carcinoma cells (HepG2), providing information regarding the hepatotoxicity of these compounds (Table 3). The SIs of compounds 8 and 12 are both >100, as expected for antimalarial lead compounds, tested here in parallel under similar conditions ($IC_{50HepG2}$ 84 and >460 μM for compounds 12 and 8, respectively), with compound 8 showing a selectivity of >2,000. The treatment of *P. falciparum* parasites with compounds 8 and 12 affected parasite proliferation within the first growth cycle (first 24 h), similar to that observed for compound 1. The inhibition of

TABLE 3 *In vitro* selectivity indexes of compound 1 and candidate molecules 4 and 7 identified in this work[a]

Antimalarial	*In vitro* antimalarial activity			*In vitro* antitoxoplasmic activity	
	$IC_{50(3D7)}$ (M)	SI [$IC_{50(K\text{-}562)}$/ $IC_{50(3D7)}$]	SI [$IC_{50(HepG2)}$/ $IC_{50(3D7)}$]	$IC_{50(RH)}$ (M)	SI [$IC_{50(K\text{-}562)}$/ $IC_{50(RH)}$]
Compound 1	1.45×10^{-6}	13.72	ND[b]	4.80×10^{-6}	3.43
Chloroquine	1.03×10^{-8}	1,068	ND		
Artemisinin	2.87×10^{-8}	3,484	ND		
Artesunate	9.70×10^{-9}	109	ND		
Triclosan	1.55×10^{-6}	8.65	ND	3.20×10^{-7}	41.87
Compound 8	2.30×10^{-7}	1,078	>2,000		
Compound 12	1.80×10^{-7}	74	469		
Compound 4				1.81×10^{-7}	488
Compound 7				2.00×10^{-7}	275

[a] The selectivity index (SI) is defined as the ratio of the IC_{50} value determined on a human cell model (cytotoxicity) to the IC_{50} value determined on *P. falciparum* (antiplasmodial activity) or *Toxoplasma gondii*. K-562 erythroblasts, HepG2 human hepatocellular carcinoma cells, *P. falciparum* 3D7, and *T. gondii* RH strains were selected as standards for comparison. The SIs of other antimalarials were also determined.
[b] ND, not determined.

Plasmodium by compound 12, supplied at a 2× IC_{50}, was irreversible after a 12-h incubation (not shown). Taken together, these data show that the exploration of the chemical space of piperidinyl-benzimidazolone analogs led to the identification of compounds with *in vitro* properties comparable to those of validated antiparasitic molecules currently used in therapeutic treatments, although their *in vivo* efficacy still needs to be improved.

Interactions of compounds 8 and 12 with artemisinin in *in vitro* trials against *P. falciparum*. We used isobolograms to evaluate the *in vitro* interaction of two of the compounds acting against *P. falciparum*, i.e., compounds 8 and 12, with the front-line antimalarial artemisinin. To that end, *P. falciparum* was incubated with compound-artemisinin combinations described in Materials and Methods. Concentrations of each compound were expressed as fractional inhibitory concentrations (FIC), i.e., the fraction of the IC_{50}s of compounds when tested alone. The isobolograms in Fig. 5 show that interaction of compounds 8 and 12 with artemisinin were similar: under all conditions, the summed FIC (ΣFIC) measured for each compound-artemisinin combination was close to 1.0 or slightly higher. None of the ΣFICs were >2.0, which is regarded as a cutoff for antagonism (37–39). These results indicate that the interaction between compound 8 or 12 and artemisinin is additive.

Analysis of the structure-activity relationship of compounds with *in vitro* antiproliferating activity against *T. gondii* and *P. falciparum*. Figure 6 summarizes the structure-activity relationship (SAR) trends that can be deduced from the chemical structures of compounds, their *in vitro* pharmacological activities against *T. gondii* or *P. falciparum*, and their low *in vitro* adverse effects on human K-562 cells. Here, we propose two distinct SAR models, one for each of the tested *Apicomplexa* parasites, which have shared but also diverging features.

Considering parts A and B, only a few changes could be made that would lead to beneficial effects. Part A was modulated with a complete substitution of the benzimidazolone by a 1-phenyl-1,3,8-triazaspiro[4,5]decan-4-one scaffold (a substructure found in VU0285655, a specific inhibitor of PLD2) and still exhibited antitoxoplasmic properties (Fig. 6a). In contrast, its antimalarial property was improved when part A was substituted with phenylsulfonamide or phenylbenzenesulfonamide (Fig. 6b). At the level of part B, although the piperidine cycle was essential for the effects against *Plasmodium*, some modifications could be made without decreasing the antitoxoplasmic properties, as long as only one N atom was present and no double bonds were added (Fig. 6b). Parts A and B are critical for the molecular mode of action of galvestine-1 and halopemide at the level of their respective enzymatic targets. The importance of the structural motifs in parts A and B in the antiparasitic activities is therefore consistent with interference with a glycerolipid-manipulating system.

Part C was important in both *T. gondii* and *P. falciparum*, leading to a complete loss of antiparasitic activity when absent from the piperidinyl-benzimidazolone scaffold. Aromatic cycles were beneficial over different hydrophobic groups, like alkyl chains. When considering the effects on *Plasmodium*, the dibenzylamido ethoxy group appeared to be essential (Fig. 6b), whereas modulations were possible relative to the effects against *Toxoplasma*. This difference suggests that selectivity on *P. falciparum* is partly due to the dibenzylamido ethoxy motif, which was not initially thought to interfere with glycerolipid-manipulating enzymes (40), and this feature suggests that off- or promiscuous target(s) might be responsible for part of the effect on the malaria parasite. Compounds with a part C similar to that of VU0285655 were efficient against *Plasmodium* in spite of the absence of a PLD2, indicating that the dibenzylamido ethoxy group might be avoided to limit possible effects on undesired targets.

Therefore, the SAR analyses indicate that compounds with improved efficacies after changes in parts A and B are consistent with changes in selectivity on targets possibly acting in glycerolipid metabolism, and that SAR in part C should be refined, especially relative to the antimalarial activity.

DISCUSSION

Previous analyses of piperidinyl-benzimidazolone analogs have shown that this chemotype is a novel source for identifying compounds acting specifically on enzymes manipulating DAG (like plant MGD enzymes) (23, 40) or PC/PA (like human PLDs) (41, 42) (Fig. 1). The mode of action of these compounds involves their binding at the level of the substrate-binding and/or catalytic sites, and at least in one case, it was shown that inhibition was due to competition with the binding of the DAG structure (23). The two-dimensional chemical structure of the piperidinyl-benzimidazolone chemotype has no obvious similarity with the DAG-PA structure (see Fig. 1); nevertheless, three-dimensional modeling of galvestine-1 and DAG has shown that part of the structures of

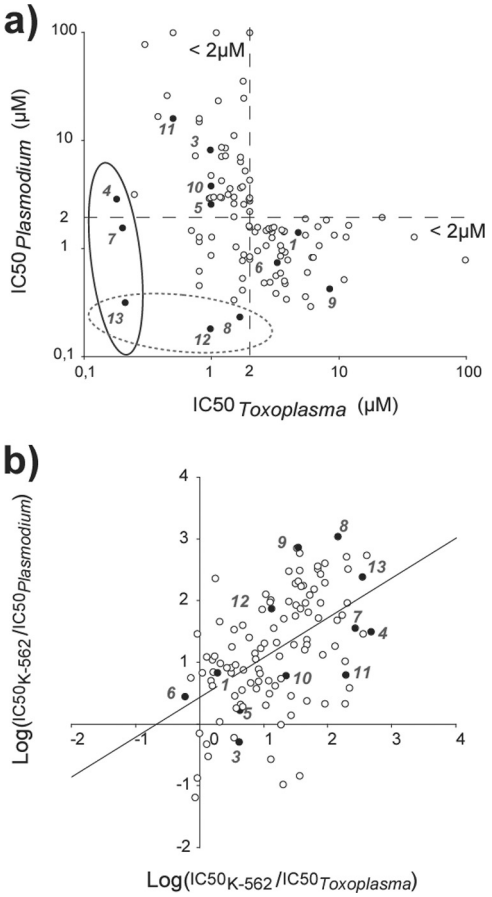

FIG 4 Two-step exploration of the library of piperidinyl-benzimidazolone analogs. (a) Step 1: selection of compounds inhibiting *T. gondii* or *P. falciparum in vitro* proliferation with an IC_{50} of ≤2 μM. The effects of all 250 compounds on the *in vitro* proliferation of both parasites were determined via IC_{50} measurement. The corresponding IC_{50}s (see Table S1 in the supplemental material) were used to select 114 compounds having an *in vitro* antiparasitic efficacy with an IC_{50} of ≤2 μM on at least one parasitic model to perform subsequent analyses. The graph highlights compounds acting with the lowest IC_{50}s against *T. gondii* (circled in solid line) or *P. falciparum* (circled in dotted line). (b) Step 2, analyses of the selectivity indexes. The selectivity index (SI) is defined as the ratio of the IC_{50} value determined on a human cell model (cytotoxicity) to the IC_{50} value determined on *P. falciparum* or *T. gondii*. We selected K-562 erythroblasts, *P. falciparum* 3D7, and *T. gondii* RH strains as standards for comparisons. The numbers and respective closed circles correspond to the compounds illustrated in Fig. 2.

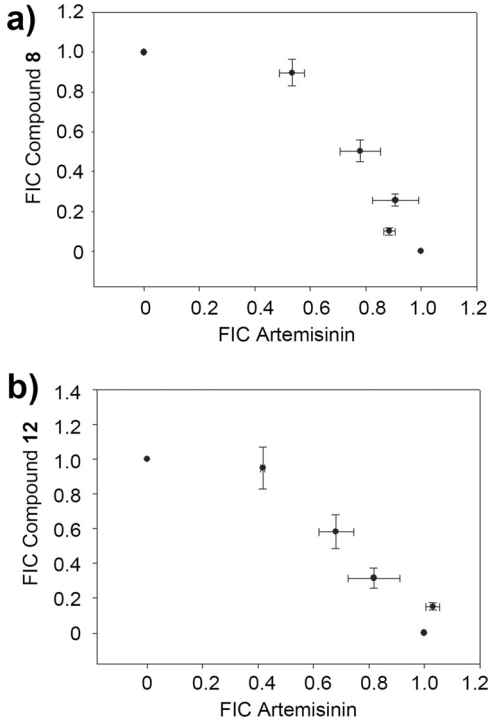

FIG 5 Isobolograms showing the antimalarial additivity between compounds 8 (a) or 12 (b) and artemisinin. The compound concentrations are expressed as the fractional inhibitory concentration (FIC). For each compound-artemisinin combination, ΣFIC values need to be <0.5 or >2 to represent synergism or antagonism, respectively (see Materials and Methods). Both isobolograms indicate neutral interactions. The data are averaged from 3 independent experiments, each carried out in triplicate. The error bars represent the standard error of the mean (SEM).

the inhibitors might superimpose the glycerol moiety of the DAG structure, using superimposed H-bond acceptors (23).

In *Apicomplexa*, neither the target for galvestine-1 (MGDG synthases or MGDs) nor that of halopemide and VU0285655 (PLDs) has been identified. No genes coding for MGDs or PLDs were identified in the genomes of the parasites. Considering MGDs, the incorporation of radiolabeled galactose from UDP-galactose into a lipid having chromatographic properties similar to those of MGDG has been reported in *T. gondii*- and *P. falciparum*-permeabilized cells (49) but was not detected in *P. falciparum* microsomes (50). The actual presence of MGDG in these parasites was not detected by sensitive mass spectrometry (15, 51). In the absence of any clear homolog gene, it is thus likely that plastid MGDG synthases have been lost or have strongly diverged in the course of the *Apicomplexa* evolution. Considering PLDs, the apparent lack of this phospholipase class is puzzling, since this enzyme might be a tool for diverting and scavenging glycerolipids from the host cell. Other protein candidates, among which PA-synthesizing acyltransferases, PAPs, DGKs, PLCs, phospholipase A2s (PLA2s), and virtually all enzymes synthesizing phospholipid classes might manipulate DAG-PA structures in *Apicomplexa* cells. In addition, since DAG, PA, and some phospholipids are not only metabolites but also secondary messengers, possible targets include DAG- and PA-activated proteins.

The library of compounds we explored contains all the structural motifs that have proven to be essential for driving galvestine-1, halopemide, and VU0285655 specificity, including the 1-phenyl-1,3,8-triazaspiro[4,5]decan-4-one scaffold and intense changes at the level of piperidinyl-benzimidazolone moiety (Fig. 2). Since the rationale for this study was to attempt to interfere with a process occurring in the core of biomembranes, the presence of a hydrophobic part (part C) to promote a partitioning of the compounds inside the membrane phase was also investigated by substitution with other cyclic structures and alkyl chains.

Our preliminary analysis of the effects of compound 1 on parasite and human cell models has shown that this compound acts on both parasites (*T. gondii* and *P. falciparum*), with IC_{50}s in the 1 to 10 μM range. In *T. gondii*, compound 1 interfered specifically with cell division. This first set of results (Fig. 3a and b) supports that compound 1 acts on parasite multiplication, which is expected if membrane biogenesis was targeted. In *Plasmodium*, compound 1 inhibited the proliferation of parasites in red blood

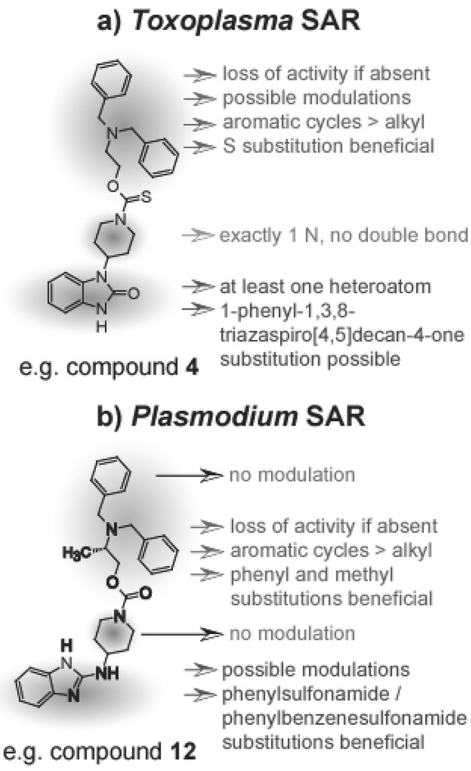

FIG 6 Structure-activity relationship (SAR) analysis of compounds acting more specifically on *T. gondii* and on *P. falciparum*. SAR trends were deduced from the activities of compounds on the *in vitro* proliferation of parasites and on human cells, including IC_{50} and SI values. (a) SAR model correlating the structure of tested compounds with the efficacy on *T. gondii*. SAR trends are illustrated using the structure of compound 4. (b) SAR model correlating the structure of tested compounds with the efficacy on *P. falciparum*. SAR trends are illustrated using the structure of compound 12. No modulation, changes of the group lead to a partial or total loss of biological activity.

cells regardless of the erythrocytic stage (Fig. 3c and d). The effect of compound 1 was incompatible with a delayed death phenotype and thus seemed to rule out an impairment of apicoplast maintenance (Fig. 3c and d). Piperidinyl-benzimidazolones might act on lipid metabolism occurring in another compartment, with the ER being a likely target. The synthesis of analogs associated with a fluorescent probe and localization study may reveal the site of action of piperidinyl-benzimidazolones.

Compound 1 showed an efficacy on all tested strains of chloroquine-sensitive and chloroquine-resistant strains of *P. falciparum* (Table 1). The *in vitro* toxic effects in human cells were determined to be in the 15 to 200 μM range (Table 2). Using K-562 human erythrocytes as a standard, we estimated a selectivity index (SI) for subsequent comparisons of the compounds (Table 3).

We explored the 250-compound library of piperidinyl-benzimidazolone analogs in two steps. After selection of 114 compounds with IC_{50}s of ≤2 μM against at least one of the tested parasites (Fig. 4a), we determined the effects on K-562 cells, allowing for comparisons of the SIs (Fig. 4b). A weak linear correlation was detected between the SIs determined relative to each parasite (Fig. 4b) (linear correlation: $y = 0.6429x + 0.4342$; $R^2 = 0.256$). This indicates that a structural correlation exists in compounds acting on both *Apicomplexa* models but that species-specific structures likely exist. Indeed, compounds 4 and 7 appear to be more specific against *T. gondii*, while compounds 8 and 12 are more efficient against *P. falciparum* (Fig. 4a). When tested on the *in vitro* proliferation of *Eimeria tenella* infecting bovine MDBK cells, we did not detect any antiparasitic effect of compound 8 <100 μM. Compound 12 had *in vitro* inhibitory effects on *Eimeria*, with an IC_{50} in the 1 to 2 μM range and no cytotoxicity on Madin-Darby bovine kidney (MDBK) cells at these concentrations (not shown). These results support species-specific properties within the *Apicomplexa* phylum. This study also highlighted compounds with an improved SI compared to that of compound 1, with SIs of 488 for compound 4 and 275 for compound 7 against *T. gondii*, and SIs of 1,078 for compound 8 and 74 for compound 12 against *P. falciparum*. These SIs are in the range of those measured for the other drugs we tested in parallel, such as chloroquine (SI, 1,068) or artesunate (SI, 109) (Table 3).

As part of our strategy to develop new molecules for therapeutic intervention, we assessed the toxicities of the two best compounds, 8 and 12, acting against *Plasmodium*. BALB/c mice received four daily injections at 50 mg · kg of body weight^{-1}. No toxic effect was observed after ≥20 days after the first injection (not shown), correlating with the low *in vitro* toxicities of these molecules. A similar experiment was conducted on BALB/c mice infected by *Plasmodium vinckei* and treated at 25 mg · kg^{-1} in a 4-day injection trial (52, 53). Parasitemia following treatment with compound 12 was significantly reduced on days 3 and 4 (see Fig. S2 in the supplemental material). However, no curative effect was observed. This assay suggests that compound 12 limits the proliferation of parasites *in vivo* and delays parasitemia, but the molecule properties should be further optimized to reach a complete cure. Such limited *in vivo* activities are not uncommon for a trial based on the initial formulation of a candidate drug. They should guide the design of new analogs with antimalarial activity based on the compound 12 scaffold. Isobole analyses of the interaction of compounds 8 and 12 with artemisinin (Fig. 5) indicate that the interaction is additive. It is thus possible to explore the potential benefits of these compounds in artemisinin-based combination therapies (ACTs).

We performed a preliminary proteomic analysis in order to identify possible target proteins in *P. falciparum* (described in the supplemental material). We based our analysis on a piperidinyl-benzimidazolone analog, which is linked to biotin. We grafted this analog to a NeutrAvidin matrix and chromatographed red blood cells (mock) or *P. falciparum* protein extracts, focusing on soluble and insoluble proteins in parallel experiments. We then analyzed the proteomic profiles of the proteins bound to the affinity matrix by mass spectrometry. In the mock (red blood cell) trials, we detected only a very low level of hemoglobin contaminant together with avidin released from the affinity matrix. In the *P. falciparum* extract, we detected 12 major polypeptides, including a protein acting on an acyl-containing substrate (a substructure also found in diacylglycerol and phosphatidic acid), a pyruvate kinase (acting in the pyruvate hub upstream of fatty acid synthesis), an enzyme manipulating glycerone-P and glyceraldehyde-3-P, which are close to the glycerol backbones of diacylglycerol and phosphatidic acid. We also detected proteins of unknown function. Based on these experiments, we obtained a list of putative proteins binding the biotinylated compound, which should be characterized in greater detail in the future to check if they are also inhibited and if the genetic impairment is lethal. Additional proteins eluted from

the affinity matrix have been detected in smaller amounts and shall be also analyzed.

Taken together, *in vitro* and *in vivo* trials reported in this article indicate that we refined compound structures, which consistently had a possible effect on membrane glycerolipids, and that we gained in *in vitro* efficacy reaching the range of the antiparasitic drugs tested in parallel. In-depth analyses of the biological response of parasites should be undertaken to provide clues on the cellular modes of action of these novel drugs. More improvements should be made to develop molecules acting *in vivo* in mono- or multitherapies. Future developments should therefore benefit from the SAR models we proposed here.

ACKNOWLEDGMENTS

This work was supported by Oséo-Anvar, Conseil Régional Rhône-Alpes (PhD grant allocated to N.S.), Agence Nationale de la Recherche (PlasmoExplore, PlasmoExpress, ReGal, and DiaDomOil grants allocated to E.M.), the European Commission (FP7 OIF Marie Curie Fellowship, project Apicolipid, allocated to C.Y.B.), Labex GRAL (to E.M.), and a joint program of the French Ministry of Foreign Affairs and the South African Department of Sciences and Technologies (E.M. and L.-M.B.).

We thank Ricardo Mondragon for advice on gliding assays, Lauriane Kuhn and the EDyP laboratory for proteomic analyses presented in the supplemental material, and Christian Vincent and Dean Goodman for fruitful discussions.

REFERENCES

1. **Morrison DA.** 2009. Evolution of the *Apicomplexa*: where are we now? Trends Parasitol. **25:**375–382. http://dx.doi.org/10.1016/j.pt.2009.05.010.
2. **WHO.** 2011. World malaria report: 2011. World Health Organization, Geneva, Switzerland. http://www.who.int/malaria/publications/atoz/9789241564403/en/.
3. **Sukthana Y.** 2006. Toxoplasmosis: beyond animals to humans. Trends Parasitol. **22:**137–142. http://dx.doi.org/10.1016/j.pt.2006.01.007.
4. **Limenitakis J, Soldati-Favre D.** 2011. Functional genetics in *Apicomplexa*: potentials and limits. FEBS Lett. **585:**1579–1588. http://dx.doi.org/10.1016/j.febslet.2011.05.002.
5. **Tarun AS, Vaughan AM, Kappe SH.** 2009. Redefining the role of *de novo* fatty acid synthesis in *Plasmodium* parasites. Trends Parasitol. **25:**545–550. http://dx.doi.org/10.1016/j.pt.2009.09.002.
6. **Dechamps S, Shastri S, Wengelnik K, Vial HJ.** 2010. Glycerophospholipid acquisition in *Plasmodium*—a puzzling assembly of biosynthetic pathways. Int. J. Parasitol. **40:**1347–1365. http://dx.doi.org/10.1016/j.ijpara.2010.05.008.
7. **Mi-Ichi F, Kita K, Mitamura T.** 2006. Intraerythrocytic *Plasmodium falciparum* utilize a broad range of serum-derived fatty acids with limited modification for their growth. Parasitology **133:**399–410. http://dx.doi.org/10.1017/S0031182006000540.
8. **Mazumdar J, Striepen B.** 2007. Make it or take it: fatty acid metabolism of apicomplexan parasites. Eukaryot. Cell **6:**1727–1735. http://dx.doi.org/10.1128/EC.00255-07.
9. **Botté CY, Dubar F, McFadden GI, Maréchal E, Biot C.** 2012. *Plasmodium falciparum* apicoplast drugs: targets or off-targets? Chem. Rev. **112:**1269–1283. http://dx.doi.org/10.1021/cr200258w.
10. **Santiago TC, Zufferey R, Mehra RS, Coleman RA, Mamoun CB.** 2004. The *Plasmodium falciparum* PfGatp is an endoplasmic reticulum membrane protein important for the initial step of malarial glycerolipid synthesis. J. Biol. Chem. **279:**9222–9232. http://dx.doi.org/10.1074/jbc.M310502200.
11. **Dubots E, Botté C, Boudière L, Yamaryo-Botté Y, Jouhet J, Maréchal E, Block MA.** 2012. Role of phosphatidic acid in plant galactolipid synthesis. Biochimie **94:**86–93. http://dx.doi.org/10.1016/j.biochi.2011.03.012.
12. **Raabe A, Berry L, Sollelis L, Cerdan R, Tawk L, Vial HJ, Billker O, Wengelnik K.** 2011. Genetic and transcriptional analysis of phosphoinositide-specific phospholipase C in *Plasmodium*. Exp. Parasitol. **129:**75–80. http://dx.doi.org/10.1016/j.exppara.2011.05.023.
13. **Fang JM, Marchesini N, Moreno SNJ.** 2006. A *Toxoplasma gondii* phosphoinositide phospholipase C (TgPI-PLC) with high affinity for phosphatidylinositol. Biochem. J. **394:**417–425. http://dx.doi.org/10.1042/BJ20051393.
14. **Botté CY, Yamaryo-Botté Y, Janouskovec J, Rupasinghe T, Keeling PJ, Crellin P, Coppel RL, Maréchal E, McConville MJ, McFadden GI.** 2011. Identification of plant-like galactolipids in *Chromera velia*, a photosynthetic relative of malaria parasites. J. Biol. Chem. **286:**29893–29903. http://dx.doi.org/10.1074/jbc.M111.254979.
15. **Botté C, Saïdani N, Mondragon R, Mondragón M, Isaac G, Mui E, McLeod R, Dubremetz JF, Vial H, Welti R, Cesbron-Delauw MF, Mercier C, Maréchal E.** 2008. Subcellular localization and dynamics of a digalactolipid-like epitope in *Toxoplasma gondii*. J. Lipid Res. **49:**746–762. http://dx.doi.org/10.1194/jlr.M700476-JLR200.
16. **Botté CY, Yamaryo-Botté Y, Rupasinghe TW, Mullin KA, MacRae JI, Spurck TP, Kalanon M, Shears MJ, Coppel RL, Crellin PK, Maréchal E, McConville MJ, McFadden GI.** 2013. Atypical lipid composition in the purified relict plastid (apicoplast) of malaria parasites. Proc. Natl. Acad. Sci. U. S. A. **110:**7506–7511. http://dx.doi.org/10.1073/pnas.1301251110.
17. **MacRae JI, Maréchal E, Biot C, Botté CY.** 2012. The apicoplast: a key target to cure malaria. Curr. Pharm. Des. **18:**3490–3504. http://dx.doi.org/10.2174/138161212801327275.
18. **Min Y, Kumar TRS, Nkrumah LJ, Coppi A, Retzlaff S, Li CD, Kelly BJ, Moura PA, Lakshmanan V, Freundlich JS, Valderramos JC, Vilcheze C, Siedner M, Tsai JHC, Falkard B, Sidhu AbS, Purcell LA, Gratraud P, Kremer L, Waters AP, Schiehser G, Jacobus DP, Janse CJ, Ager A, Jacobs WR, Jr, Sacchettini JC, Heussler V, Sinni P, Fidock DA.** 2008. The fatty acid biosynthesis enzyme FabI plays a key role in the development of liver-stage malarial parasites. Cell Host Microbe **4:**567–578. http://dx.doi.org/10.1016/j.chom.2008.11.001.
19. **Vaughan AM, O'Neill MT, Tarun AS, Camargo N, Phuong TM, Aly AS, Cowman AF, Kappe SH.** 2009. Type II fatty acid synthesis is essential only for malaria parasite late liver stage development. Cell. Microbiol. **11:**506–520. http://dx.doi.org/10.1111/j.1462-5822.2008.01270.x.
20. **Wengelnik K, Vidal V, Ancelin ML, Cathiard AM, Morgat JL, Kocken CH, Calas M, Herrera S, Thomas AW, Vial HJ.** 2002. A class of potent antimalarials and their specific accumulation in infected erythrocytes. Science **295:**1311–1314. http://dx.doi.org/10.1126/science.1067236.
21. **Caldarelli SA, Hamel M, Duckert JF, Ouattara M, Calas M, Maynadier M, Wein S, Périgaud C, Pellet A, Vial HJ, Peyrottes S.** 2012. Disulfide prodrugs of albitiazolium (T3/SAR97276): synthesis and biological activities. J. Med. Chem. **55:**4619–4628. http://dx.doi.org/10.1021/jm3000328.
22. **González-Bulnes P, Bobenchik AM, Augagneur Y, Cerdan R, Vial HJ, Llebaria A, Ben Mamoun C.** 2011. PG12, a phospholipid analog with potent antimalarial activity, inhibits *Plasmodium falciparum* CTP: phosphocholine cytidylyltransferase activity. J. Biol. Chem. **286:**28940–28947. http://dx.doi.org/10.1074/jbc.M111.268946.
23. **Botté CY, Deligny M, Roccia A, Bonneau AL, Saïdani N, Hardré H, Aci S, Yamaryo-Botté Y, Jouhet J, Dubots E, Loizeau K, Bastien O, Bréhélin L, Joyard J, Cintrat JC, Falconet D, Block MA, Rousseau B, Lopez R, Maréchal E.** 2011. Chemical inhibitors of monogalactosyldiacylglycerol synthases in *Arabidopsis thaliana*. Nat. Chem. Biol. **7:**834–842. http://dx.doi.org/10.1038/nchembio.658.
24. **Morisaki JH, Heuser JE, Sibley LD.** 1995. Invasion of *Toxoplasma gondii* occurs by active penetration of the host cell. J. Cell Sci. **108**(Pt 6):2457–2464.
25. **McFadden DC, Seeber F, Boothroyd JC.** 1997. Use of *Toxoplasma gondii* expressing beta-galactosidase for colorimetric assessment of drug activity *in vitro*. Antimicrob. Agents Chemother. **41:**1849–1853.
26. **Seeber F, Boothroyd JC.** 1996. *Escherichia coli* beta-galactosidase as an *in vitro* and *in vivo* reporter enzyme and stable transfection marker in the intracellular protozoan parasite *Toxoplasma gondii*. Gene **169:**39–45. http://dx.doi.org/10.1016/0378-1119(95)00786-5.
27. **Conseil V, Soête M, Dubremetz JF.** 1999. Serine protease inhibitors block invasion of host cells by *Toxoplasma gondii*. Antimicrob. Agents Chemother. **43:**1358–1361.
28. **Håkansson S, Morisaki H, Heuser J, Sibley LD.** 1999. Time-lapse video microscopy of gliding motility in *Toxoplasma gondii* reveals a novel, biphasic mechanism of cell locomotion. Mol. Biol. Cell **10:**3539–3547. http://dx.doi.org/10.1091/mbc.10.11.3539.
29. **Rodriguez C, Afchain D, Capron A, Dissous C, Santoro F.** 1985. Major surface protein of *Toxoplasma gondii* (p30) contains an immunodominant region with repetitive epitopes. Eur. J. Immunol. **15:**747–749. http://dx.doi.org/10.1002/eji.1830150721.
30. **Darcy F, Maes P, Gras-Masse H, Auriault C, Bossus M, Deslee D,**

Godard I, Cesbron MF, Tartar A, Capron A. 1992. Protection of mice and nude rats against toxoplasmosis by a multiple antigenic peptide construction derived from *Toxoplasma gondii* P30 antigen. J. Immunol. **149:** 3636–3641.
31. **Mondragon R, Frixione E.** 1996. Ca(2+)-dependence of conoid extrusion in *Toxoplasma gondii* tachyzoites. J. Eukaryot. Microbiol. **43:**120–127. http://dx.doi.org/10.1111/j.1550-7408.1996.tb04491.x.
32. **Carruthers VB, Moreno SN, Sibley LD.** 1999. Ethanol and acetaldehyde elevate intracellular [Ca2+] and stimulate microneme discharge in *Toxoplasma gondii*. Biochem. J. **342**(Pt 2)**:**379–386.
33. **Charif H, Darcy F, Torpier G, Cesbron-Delauw MF, Capron A.** 1990. *Toxoplasma gondii*: characterization and localization of antigens secreted from tachyzoites. Exp. Parasitol. **71:**114–124. http://dx.doi.org/10.1016/0014-4894(90)90014-4.
34. **Trager W, Jensen JB.** 1976. Human malaria parasites in continuous culture. Science **193:**673–675. http://dx.doi.org/10.1126/science.781840.
35. **Desjardins RE, Pamplin CL, III, von Bredow J, Barry KG, Canfield CJ.** 1979. Kinetics of a new antimalarial, mefloquine. Clin. Pharmacol. Ther. **26:**372–379.
36. **van Schalkwyk DA, Priebe W, Saliba KJ.** 2008. The inhibitory effect of 2-halo derivatives of D-glucose on glycolysis and on the proliferation of the human malaria parasite *Plasmodium falciparum*. J. Pharmacol. Exp. Ther. **327:**511–517. http://dx.doi.org/10.1124/jpet.108.141929.
37. **Bell A.** 2005. Antimalarial drug synergism and antagonism: mechanistic and clinical significance. FEMS Microbiol. Lett. **253:**171–184. http://dx.doi.org/10.1016/j.femsle.2005.09.035.
38. **Odds FC.** 2003. Synergy, antagonism, and what the chequerboard puts between them. J. Antimicrob. Chemother. **52:**1. http://dx.doi.org/10.1093/jac/dkg301.
39. **Johnson MD, MacDougall C, Ostrosky-Zeichner L, Perfect JR, Rex JH.** 2004. Combination antifungal therapy. Antimicrob. Agents Chemother. **48:**693–715. http://dx.doi.org/10.1128/AAC.48.3.693-715.2004.
40. **Boudière L, Botté C, Saidani N, Lajoie M, Marion J, Bréhélin L, Yamaryo-Botté Y, Satiat-Jeunemaître B, Breton C, Girard-Egrot A, Bastien O, Jouhet J, Falconet D, Block MA, Maréchal E.** 2012. Galvestine-1, a novel chemical probe for the study of the glycerolipid homeostasis system in plant cells. Mol. Biosyst. http://dx.doi.org/10.1039/c2mb25067e.
41. **Monovich L, Mugrage B, Quadros E, Toscano K, Tommasi R, LaVoie S, Liu E, Du Z, LaSala D, Boyar W, Steed P.** 2007. Optimization of halopemide for phospholipase D2 inhibition. Bioorg. Med. Chem. Lett. **17:**2310–2311. http://dx.doi.org/10.1016/j.bmcl.2007.01.059.
42. **Scott SA, Selvy PE, Buck JR, Cho HP, Criswell TL, Thomas AL, Armstrong MD, Arteaga CL, Lindsley CW, Brown HA.** 2009. Design of isoform-selective phospholipase D inhibitors that modulate cancer cell invasiveness. Nat. Chem. Biol. **5:**108–117. http://dx.doi.org/10.1038/nchembio.140.
43. **Selvy PE, Lavieri RR, Lindsley CW, Brown HA.** 2011. Phospholipase D: enzymology, functionality, and chemical modulation. Chem. Rev. **111:** 6064–6119. http://dx.doi.org/10.1021/cr200296t.
44. **He CY, Shaw MK, Pletcher CH, Striepen B, Tilney LG, Roos DS.** 2001. A plastid segregation defect in the protozoan parasite *Toxoplasma gondii*. EMBO J. **20:**330–339. http://dx.doi.org/10.1093/emboj/20.3.330.
45. **Goodman CD, Su V, McFadden GI.** 2007. The effects of anti-bacterials on the malaria parasite *Plasmodium falciparum*. Mol. Biochem. Parasitol. **152:**181–191. http://dx.doi.org/10.1016/j.molbiopara.2007.01.005.
46. **Dahl EL, Rosenthal PJ.** 2008. Apicoplast translation, transcription and genome replication: targets for antimalarial antibiotics. Trends Parasitol. **24:**279–284. http://dx.doi.org/10.1016/j.pt.2008.03.007.
47. **Dahl EL, Rosenthal PJ.** 2007. Multiple antibiotics exert delayed effects against the *Plasmodium falciparum* apicoplast. Antimicrob. Agents Chemother. **51:**3485–3490. http://dx.doi.org/10.1128/AAC.00527-07.
48. **Vial HJ, Thuet MJ, Philippot JR.** 1982. Phospholipid biosynthesis in synchronous *Plasmodium falciparum* cultures. J. Protozool. **29:**258–263. http://dx.doi.org/10.1111/j.1550-7408.1982.tb04023.x.
49. **Maréchal E, Azzouz N, de Macedo CS, Block MA, Feagin JE, Schwarz RT, Joyard J.** 2002. Synthesis of chloroplast galactolipids in apicomplexan parasites. Eukaryot. Cell **1:**653–656. http://dx.doi.org/10.1128/EC.1.4.653-656.2002.
50. **Ramasamy R, Field MC.** 2012. Terminal galactosylation of glycoconjugates in *Plasmodium falciparum* asexual blood stages and *Trypanosoma brucei* bloodstream trypomastigotes. Exp. Parasitol. **130:**314–320. http://dx.doi.org/10.1016/j.exppara.2012.02.017.
51. **Welti R, Mui E, Sparks A, Wernimont S, Isaac G, Kirisits M, Roth M, Roberts CW, Botté C, Maréchal E, McLeod R.** 2007. Lipidomic analysis of *Toxoplasma gondii* reveals unusual polar lipids. Biochemistry **46:** 13882–13890. http://dx.doi.org/10.1021/bi7011993.
52. **Peters W.** 1975. The chemotherapy of rodent malaria, XXII. The value of drug-resistant strains of *P. berghei* in screening for blood schizontocidal activity. Ann. Trop. Med. Parasitol. **69:**155–171.
53. **Peters W, Robinson BL.** 1992. The chemotherapy of rodent malaria. XLVII. Studies on pyronaridine and other Mannich base antimalarials. Ann. Trop. Med. Parasitol. **86:**455–465.